Simulating Forest Fire Plume Dispersion, Chemistry, and Aerosol Formation Using SAM-ASP version 1.0

Chantelle R. Lonsdale[1], Matthew J. Alvarado[1], Anna L. Hodshire[2], Emily Ramnarine[2] and Jeffrey R. Pierce[2]

[1]Atmospheric and Environmental Research (AER), Lexington, MA, 02421, USA
5 [2]Department of Atmospheric Science, Colorado State University, Fort Collins, CO, 80523, USA

Correspondence to: Chantelle R. Lonsdale (clonsdal@aer.com)

Abstract. Biomass burning is a major source of trace gases and aerosols that can ultimately impact health, air quality, and climate. Global and regional-scale three-dimensional Eulerian chemical transport models (CTMs) use estimates of the primary emissions

10 from fires and can unphysically mix them across large-scale grid boxes, leading to incorrect estimates of the impact of biomass burning events. On the other hand, plume-scale process models allow for explicit simulation and examination of the chemical and physical transformations of trace gases and aerosols within biomass burning smoke plumes, and they may be used to develop parameterizations of this aging process for coarser grid-scale models. Here we describe the coupled SAM-ASP plume-scale process model, which consists of coupling the large-eddy simulation model, the System for Atmospheric Modelling (SAM), with the

15 detailed gas and aerosol chemistry model, the Aerosol Simulation Program (ASP). We find that the SAM-ASP version 1.0 model is able to correctly simulate the dilution of CO in a California chaparral smoke plume, as well as the chemical loss of NO_x, HONO, and NH_3 within the plume, the formation of PAN and O_3, the loss of OA, and the change in the size distribution of aerosols as compared to measurements and previous single-box model results. The newly coupled model is able to capture the cross-plume vertical and horizontal concentration gradients as the fire plume evolves downwind of the emission source. The integration and

20 evaluation of SAM-ASP version 1.0 presented here will support the development of parameterizations of near-source biomass burning chemistry that can be used to more accurately simulate biomass burning chemical and physical transformations of trace gases and aerosols within coarser grid-scale CTMs.

1 Introduction

Outdoor biomass burning—including wildfires, prescribed fires, and agricultural fires—is a major source of trace gases and

25 aerosols that impact health, air quality and climate. These health- and climate-relevant primary emissions from biomass burning include species deemed as hazardous air pollutants (HAPs), such as benzene, formaldehyde, and acetaldehyde, which themselves can cause acute health effects (Wentworth et al., 2018). In addition to the pollutants directly emitted by fires, chemistry in smoke plumes can produce ozone (O_3), which can negatively impact human health (U.S. EPA, 2013) as well as affect vegetation, water quality, soil and the ecosystems that they support (European Environmental Agency, 2018). O_3 formation can occur due to the

30 emission of nitrogen dioxide (NO_2), HONO, and volatile organic compounds (VOCs) and presence of sunlight (Baylon et al., 2018), with enhanced photolysis rates occurring most predominantly during midday, when photolysis rates are fastest. In 2012, the estimated median contribution of fires to maximum daily 8-hr average (MDA8) O_3 in Texas during the month of June was 2 ppbv, with maximum impacts of over 40 ppbv (McDonald-Buller et al., 2015). Long-range transport of fire emissions has also been found to contribute to elevated peak O_3 values in Europe (Ordóñez et al., 2010). Large uncertainties exist, however, in quantifying

35 O_3 production, which stems from uncertainties in fire emissions, combustion efficiency, meteorological patterns, chemical and photochemical reactions, and the effects of aerosols on plume chemistry and photolysis rates. Aerosols have been shown to both

increase O₃ formation (e.g. scattering particles can increase photolysis rates) as well as decrease O₃ (absorbing aerosol and black carbon-containing aerosol can reduce photolysis rates) (Baylon et al., 2018). Hence, the aerosol composition and size distribution, which varies within and between plumes (Collier et al., 2016), and the location of the aerosol within the plume (Alvarado et al., 2015) impact O₃ production. The presence of clouds also impacts photolysis rates and O₃ production (Flynn et al., 2010). All of

5   these factors remain highly variable and uncertain between different plumes.

Biomass burning also emits particulate matter (PM) that impacts air quality, health, and climate. PM impacts the climate directly by scattering or absorbing incoming solar radiation (e.g., Boucher et al., 2013) and indirectly by altering the properties of clouds (e.g., Pierce et al., 2007; Spracklen et al., 2011) with both effects depending on the particle size, mass and composition (Petters

10   and Kreidenweis, 2007; Seinfeld and Pandis, 2016). Bond et al. (2013) estimated that biomass burning emits about one third of total global primary carbonaceous aerosol emissions (black carbon (BC) and organic aerosol (OA)), with the size, mixing state, and chemical composition of the particles uncertain. A complex evolution of various organic trace-gas and aerosol compounds occurs as smoke ages, with all compounds containing a wide variety of volatility and reactivity that determine the ultimate partitioning into the gas- or particle-state, thus determining the size, mixing state and ultimately chemical composition of the evolving plume.

15   Hodshire et al. (2019a) described the wide-ranging results from laboratory and field studies of smoke plume aging, which show that measured net OA production/loss is dependent on the fuel and burning conditions, plume dispersion rates, and oxidant species and concentrations; however, no complete theory currently exists that can predict how OA will evolve in different plumes. Further understanding of the magnitude and extent of both the primary and secondary components of biomass burning emissions is thus required to fully understand the global impacts.

20

Over the last few decades, air quality regulations have resulted in a decrease in PM concentrations in the United States, as PM₂.₅ is a regulated pollutant under the Clean Air Act NAAQS. McClure and Jaffe (2018), however, analyzed PM₂.₅ measurements made at IMPROVE sites and found a positive trend in the 98th quantile of PM₂.₅ in the Northwest and a negative trend in the rest of the US, attributing the increase to wildfires in the Northwest, similar to positive trends in MODIS AOD. They determined that wildfires

25   are causing the increase in PM₂.₅ at the 98th quantile in the Northwest which could offset anthropogenic reductions in the region. O'Dell et al. (2019) and Knorr et al., (2018) combined surface observations and satellite-based smoke plume estimates and the GEOS-Chem chemical transport model (CTM) to identify trends in summer time smoke, non-smoke, and total PM₂.₅ across the US. They estimated that future PM emissions from biomass burning may exceed anthropogenic emission levels, including in densely populated areas in the eastern Europe-Russia-central Asia region. The growing relative importance of biomass burning as

30   a source of pollution increases the need to understand in-plume chemistry and physics.

Three-dimensional (3D) Eulerian CTMs make estimates of the primary emissions from fires and unphysically mix them across large-scale grid boxes, which can lead to incorrect estimates of the ultimate impact of fires on health, air quality, and climate (e.g., Alvarado et al., 2009; Sakamoto et al., 2016: Ramnarine et al., 2019; Hodshire et al., 2019b). Thus, in order to accurately predict

35   biomass burning effects on air quality and climate in regional and global models, a sub-grid scale representation of aged biomass-burning trace gas and aerosol size evolution is required. Regarding the impact of coarse-model mixing on O₃, Baker et al.(2015) found that the 3D Eulerian Community Multiscale Air Quality Model (CMAQ) tended to overestimate the impact of fires on individual hourly O₃ measurements at US Environmental Protection Agency (EPA) Clean Air Status Trends Network (CASTNET) monitoring sites near fires by up to 40 ppbv and underestimate it further downwind by up to 20 ppbv. This behavior is consistent

40   with an incorrect treatment of the sub-grid-scale, near-source O₃ and NO_y chemistry, where the model underestimates the loss of

NO_x (NO + NO_2) near the source due to formation of inorganic and organic nitrates, thus overestimating O_3 formation near the source. This same error leads to an underestimate of the amount of peroxy nitrates formed near the source, which then leads to an underestimate of O_3 formation downwind when the peroxy nitrates decompose, regenerating NO_x (Alvarado et al., 2010).

5 The initial aerosol size, number, and mass in biomass burning smoke plumes can vary with fuel type (Janhäll et al., 2010) (e.g., Boreal versus Savannah) and combustion condition (Hosseini et al., 2012) and are leading uncertainties in the predictions of PM in regional and global models (Lee et al., 2013). These inputs are often based on spatially sparse, point measurements taken at only one stage in the atmospheric lifetime of a biomass burning plume with some measurements representing fresh emissions and some representing aged emissions (Pierce et al., 2007; Janhäll et al., 2010; Akagi et al., 2011; Hodshire et al., 2019a). These sparse inputs

10 do not account for many of the non-linear physical and chemical changes that take place within a smoke plume near the fire, with the coarse grid scales of regional and global models (10s to 100s of kilometers) too large to resolve near-source smoke plume chemical and physical evolution. By accounting for sub-grid aerosol processes that occur in biomass burning plumes, such as coagulation and condensation/evaporation of organic species, the biomass burning impact on aerosol number concentration and size distribution can be better simulated (Ramnarine et al., 2019). In order to resolve aerosol processes in biomass burning plumes,

15 regional and global models thus require grid-scale-appropriate, aged aerosol emissions size distributions to accurately simulate the health and climate effects of biomass-burning aerosols in global and regional atmospheric models. Additionally, in order to better characterize the chemical processes in biomass burning plumes, improved understanding of the oxidant and radical concentrations, photolysis rates, and parameterizations of reaction rates for different classifications of smoke is needed (Hodshire et al., 2019a).

20 As an initial attempt to represent sub-grid plume chemistry and physics in coarse-grid models, Lonsdale et al. (2015) developed a parameterization of trace gas and aerosol formation in biomass burning plumes using the Aerosol Simulation Program (ASP, Alvarado et al., 2015) as a box model. ASP simulates the gas-phase, aerosol-phase, and heterogeneous chemistry of young biomass burning smoke plumes, including the formation of O_3 and secondary inorganic and organic aerosol. The ASP box-model parameterization included predicted Normalized Excess Mixing Ratios (NEMR, Akagi et al., 2011) of O_3, NO_x, PAN, and other

25 trace gases and aerosol species in terms of the fuel type, temperature, latitude, day of year, and starting hour of fire emission. Separate parameterizations were built for each fuel type, which included Savannah, Tropical Forest, Temperate Forest, and Boreal Forest. McDonald-Buller et al. (2015) used a subset of this ASP-based parameterization to adjust the chemistry of biomass burning in the Comprehensive Air Quality Model with Extensions (CAMx) and found that this approach reduced the median impact of biomass burning on MDA8 O_3 in Texas by 0.3 ppbv, or 15%. However, because the parameterization was fit to the ASP box

30 model, it did not include cross-plume gradients in trace gas and aerosol concentrations, which may be important for accurately simulating non-linear chemistry and partitioning (Garofalo et al., 2019, Hodshire et al., 2019b; Bian et al., 2017). To account for non-linear cross-plume dilution effects, Sakamoto et al. (2016) used the large-eddy simulation (LES) cloud-resolving model the System for Atmospheric Modelling (SAM; Khairoutdinov and Randall, 2003; Stevens et al., 2012), coupled with the TwO Moment Aerosol Sectional (TOMAS) microphysics module to parameterize the coagulation of aerosols in biomass burning plumes

35 (Sakamoto et al., 2015; 2016). This parameterization was used in Ramnarine et al. (2019) to investigate the impact of sub-grid coagulation on radiative forcing. However, while the SAM-TOMAS model used by Sakamoto et al. (2016) resolved plume gradients, their study did not include chemistry and phase partition. There remains a need for a modelling system that resolves plume gradients while simulating the chemical and physical processes relevant for air quality and climate.

To address the need for a dispersion-resolving model with online chemistry, partitioning, and microphysics that can help answer the biomass burning questions described above, we have developed an integrated model of ASP (Section 2.1) coupled with the SAM model (Section 2.2). We have evaluated the performance of the new model, SAM-ASP v1.0 described in Section 2.3, in simulating the measurements of CO, O_3, NO_y, and aerosols for the Williams Fire in California (Sections 3 and 4). This integrated

5 model is able to simulate both the detailed chemistry, and the horizontal and vertical dispersion affecting the near-source evolution of biomass-burning gas and aerosol chemistry and physics. Model code and inputs are publicly available as described in Section 6.

2 Models

2.1 Aerosol Simulation Program (ASP)

10 ASP (Alvarado, 2008; Alvarado and Prinn, 2009; Alvarado et al., 2009; 2015; 2016) uses a sectional aerosol size distribution representation (with the number of size bins adjustable at runtime) and includes modules to calculate aerosol thermodynamics, gas-to-aerosol mass transfer (condensation/evaporation), coagulation of aerosol particles, and aerosol optical properties. ASP has been extensively used to study the chemical and physical transformations of gases and particles within young biomass burning smoke plumes (less than 24 hours) (Alvarado and Prinn, 2009; Alvarado et al., 2009, 2010, 2015) and the optical properties of

15 smoke aerosol (Alvarado and Prinn, 2009; Alvarado et al., 2009, 2015, 2016). For example, Alvarado and Prinn (2009) used ASP to investigate the aging of biomass burning aerosol from African savannah fires sampled during the SAFARI-2000 campaign (Hobbs et al., 2003). ASP simulated the growth of the aerosol size distributions in this smoke plume and showed that coagulation had only a minor impact on the biomass burning aerosol growth in the first hour after emission. They also showed that the aerosol single scattering albedo increased in the first hour of aging from 0.87 to 0.90 and that the hygroscopicity of the aerosol decreases

20 with aging, consistent with SAFARI-2000 studies of Magi and Hobbs (2003) and Reid et al. (2005). Alvarado et al. (2015) evaluated ASP simulations for a fire in California (Williams fire; Akagi et al., 2012) and showed that ASP could accurately simulate most of the observed species (e.g., OA, O_3, NO_x, OH) using reasonable assumptions about the chemistry of the unidentified organic compounds. This method provides a chemically realistic way for determining the average chemistry of the thousands of organic compounds in the smoke plume, where an approach based on attempting to simulate the oxidation chemistry of each of these

25 compounds would be computationally intractable even if all the parameters were known. The modules of the latest version of the ASP model (ASP v2.1; Alvarado et al., 2015, 2016) used in SAM-ASP v1.0 are briefly described below.

2.1.1 Gas-Phase Chemistry

All gas-phase chemistry in ASP for organic compounds containing 4 carbons or fewer is explicitly resolved following the Leeds Master Chemical Mechanism (MCM) v3.2 (Jenkin et al., 2003). The chemical mechanism of isoprene follows the Paulot et al.

30 (2009a, b) isoprene scheme including corrections based on more recent studies (Crounse et al., 2012). The lumped chemistry for all other organic compounds follows the Regional Atmospheric Chemistry Mechanism (RACM) v2 (Goliff et al., 2013). Additional non-methane organic compounds (NMOC) species can be easily added to the mechanism. Heterogeneous reaction rates are calculated following Jacob (2000) and described in detail in Alvarado et al. (2008).

2.1.2 Aerosol Size Distribution, Thermodynamics, and Gas-Particle Mass Transfer

The aerosol size distribution in ASP is represented using a moving-center sectional approach (Jacobson, 2002). The model used here has 10 size bins with the total number of fire-emitted particles derived from multiplying the CO flux (based on measured values) by the ratio of particle number enhancement (number of particles cm^{-3}) to CO enhancement (ppb) ($\Delta N/\Delta CO = 23.7$ particles
5 cm^{-3} ppb^{-1}). We use a number mean diameter of 0.1 um, and a standard deviation of 1.9 based on the wood smoke study of Grieshop et al. (2009a, b). The current ASP SOA formation module is the semi-empirical Volatility Basis Set (VBS) model of Robinson et al. (2007) linked to the RACM2 chemical mechanism following the approach of Ahmadov et al. (2012), with the semi-volatile and intermediate-volatility organic compound (S/IVOC) chemistry expanded and optimized for biomass burning following the results of Alvarado et al. (2015), with the saturation concentration, C*, ranging from 1.0x10-2 to 1.0x106 ug m-3 at 300 K with 9 bins
10 total. Aerosol coagulation is calculated using a semi-implicit scheme (Jacobson, 2005) with a Brownian coagulation kernel. Mass transfer between the gas and aerosol phases is calculated in ASP using a hybrid scheme, where the condensation of H$_2$SO$_4$ follows the flux-limited condensation equations while the kinetic condensation/evaporation of organic species are calculated using a Gear algorithm (due to the stiff nature or kinetic OA partitioning across volatilities and particle sizes). However, NH$_3$, HNO$_3$, and HCl are assumed to be in equilibrium (Alvarado and Prinn, 2009).

2.1.3 Aerosol Optical Properties

ASP v2.1 (Alvarado et al., 2015, 2016) uses spectrally varying complex refractive indices for all aerosol components based on Hess et al. (1998). The refractive index of the inorganic aqueous solution (if present) is calculated using the molar refraction approach of Tang (1997). ASP v2.1 includes four BC mixing-rule options for the calculating absorption and scattering coefficients: (1) a volume-average dielectric constant mixing rule with BC internally mixed with other species; (2) a core-shell mixing rule,
20 where a spherical, internally mixed BC core is surrounded by a spherical shell of all other aerosol components; (3) the Maxwell Garnett mixing rule (Maxwell Garnett, 1904) with BC internally mixed with other species; and (4) an external mixture of BC and the other aerosol components. Mie calculations of aerosol optical properties for each bin of the size distribution are performed within ASP using the publicly available program DMiLay, which is based on the work of Toon and Ackerman (1981).

2.2 SAM

25 The SAM v6.10.10 model has been used to study aerosol-cloud-precipitation interactions in stratiform and convective clouds (Ovchinnikov et al., 2014; Fan et al., 2009). The standard SAM model (Khairoutdinov and Randall, 2003, http://rossby.msrc.sunysb.edu/~marat/SAM.html) includes different options of detailed cloud microphysics, as well as coupled radiation and land-surface models. SAM is able to resolve boundary layer eddies, while parameterizing smaller-scale turbulence and microphysics for the LES (vs cloud-resolving) model option. SAM can be driven by reanalysis data that includes large-scale
30 forcings, initial sounding profile, radiation heating rates, and surface fluxes. SAM has the ability to add a large amount of modeled tracer species to the cloud resolving model simulation but does not contain aerosol and chemistry packages.

2.3 SAM-ASP version 1.0 2D Lagrangian Model

We coupled ASP to the SAM model to resolve dispersing biomass burning plumes with detailed chemistry and aerosol physics. The SAM model has been previously been coupled with the TOMAS microphysics module to reproduce observed dispersion and
35 new particle formation in coal-fired power-plant plumes (Lonsdale et al., 2012; Stevens et al, 2012) and to study the coagulation

of aerosols in biomass burning plumes (Sakamoto et al., 2016). The coupling of SAM-ASP v1.0 was performed similar to the coupling of SAM and TOMAS described in Stevens et al. (2012), and the coupling of ASP to the Cloud Resolving Model (CRM6) described in Alvarado et al. (2009).

5 In this project, SAM was configured as a moving, 2D Lagrangian wall oriented normal to the mean wind direction in the layer of smoke injection (between 1200 and 1400 m in our example case shown here) as in Figure 2 from Sakamoto et al., (2016). Stevens and Pierce (2014) showed that this 2D model configuration does well in simulating SO_2 and NO_x dispersion in power-plant plumes as compared to airborne measurements. SAM was updated to transport over 600 chemical species calculated in ASP, as well as to communicate the solar zenith angle and initialize gas and aerosol tracer concentrations based on SAM meteorological parameters.

10 Photolysis rates are calculated in ASP using offline lookup tables generated by the Tropospheric Ultraviolet and Visible (TUV) radiation model (Bais et al., 2003) that depend on solar zenith angle and overhead O_3 columns. SAM-ASP v1.0 does not currently account for the impact of aerosols on these photolysis rates. ASP is run as a subroutine in each SAM master time step (10 seconds for the simulations here). The SAM model handles all tracer transport and supplies the temperature, pressure, air density, solar zenith angle, mass emissions flux, and initial gas concentrations to ASP, while ASP calculates the gas and aerosol processes within

15 each grid box. SAM-ASP v1.0 currently does not calculate deposition but may be added in the future (the plume does not contact the ground for the case described in this paper). The grid boxes in the 2D moving wall have a 500 m x 500 m horizontal resolution with a 120 km total domain width (and 500 m in the with-wind direction, 1 box) and 40 m vertical resolution with a total vertical extent of 3 km. The simulation here was spun up for 1800 s prior to emissions following Stevens and Pierce (2014). The resolution and time steps described here are flexible and should be customized depending on plume and meteorological characteristics.

20

When ASP v2.1 is run as a Lagrangian box model, it needs the initial concentrations within the plume to be specified. However, as SAM-ASP v1.0 can simulate the dispersion of the smoke horizontally and vertically, we added the capability to calculate the initial concentrations based on the mass emissions flux (kg burned m^{-2} s^{-1}), emission factors (g (kg burned)$^{-1}$), and fire area (m^2 and assumes a square shape) for biomass burning species (Akagi et al., 2011; Sakamoto et al., 2015). This allows SAM-ASP v1.0

25 to better represent a wide range of fire sizes and intensities. To reduce computation time, ASP is only called in the boxes that are impacted by smoke in each SAM timestep, defined in this study as any grid box having a concentration of CO greater than a user-defined threshold (based on background concentrations determined by ambient fire measurements).

3 Data use for example simulation

The large-scale meteorological forcing in SAM-ASP v1.0 is driven by the 3-hour, 32 km resolution North American Regional

30 Reanalysis (NARR; Mesinger et al., 2006) meteorology dataset. The fire simulated in this study to evaluate the SAM-ASP v1.0 model was a prescribed fire measured on 17 November 2009 called the Williams Fire (Akagi et al., 2012). This fire covered 81 hectares north of Buellton, CA with the fuel type classified as chaparral and the vegetation burned consisting of coastal sage scrub and scrub oak woodland understory. Surface temperatures ranged from 19 degrees C at 09:00 local time to 24 degrees C at 12:20 local time with clear skies throughout the fire duration. The plume built up gradually during the day with most of the smoke rising

35 to ~1200–1336 m above mean sea level and then drifting in a northeast direction. Two flights were conducted during the day on board a US Forest Services Twin Otter aircraft to sample initial emissions and aged smoke with an Airborne Fourier Transform Infrared Spectrometer instrument from the University of Montana taken during both flights including background measurements sampled at similar altitudes to in-plume measurements just outside the plume. Trace gas species emission factors determined as

initial emissions (within minutes of the emission source) by Akagi et al. (2012) are used to initialize ASP and included; O_3, nitrous Acid (HONO), ammonia (NH_3), ammonium (NH_4), nitric oxide (NO), NO_2, NO_x (as NO), OA and peroxy acetyl nitrate (PAN). Additional emission factors not measured, but needed to initialize ASP, were included using emission factors from Table 2 of Akagi et al. (2011), with the full list of ASP species provided in the model code repository described in Section 6. Initial aerosol

5   size distribution information is inferred from the smoke study of Grieshop et al. (2009a, b). Full details of the fire and measurements are also further described in Akagi et al. (2012). Model input background concentrations were assumed based on measurements taken outside of the defined plume. Additional static inputs required by ASP include a photolysis rate parameterization based on the time and latitude of the fire, and chemical data on aqueous phase ions and inorganics. Details of the static ASP inputs are further described in Alvarado (2008).

10   4 SAM-ASP version 1.0 Simulations of the Williams Chaparral Fire

We evaluated the performance of the newly coupled SAM-ASP v1.0 model by comparing model output to observations of the Williams Fire made by Akagi et al. (2012), which was previously simulated using ASP in a Lagrangian box model by Alvarado et al. (2015). Emission ratios for this simulation were based on observed relative background-corrected concentration close to the source from Alvarado et al. (2015) and included observed values for many gas-phase species measured by Akagi et al. (2012).

15   Plume injection height was set between 1200 to 1400 m, as this was the height at which the plume was observed to level off, where a small amount of vertical mixing can be seen as the plume ages.

The NEMR calculations were determined by calculating the average species of interest (X) and CO concentration across the plume, as was done in the measurements. The NEMR ($\Delta X/\Delta CO$ or $\Delta X/\Delta CO_2$) is then calculated relative to CO or CO_2 since they have relatively long lifetimes for the fire location, low background variability, and there were no other major nearby sources as

20   described in Akagi et al. (2012):

$$\Delta X/\Delta CO = (X_{\text{in-plume}} - X_{\text{background}}) / (CO_{\text{in-plume}} - CO_{\text{background}}) \qquad (1)$$

Averaged NEMR values over the full horizontal domain of the model for the vertical level with the peak ΔCO (and ΔCO_2) can be used to compare with aircraft observations of biomass burning plumes. Figure 1 shows a horizontal slice of the simulated ΔCO concentrations (ppbv) as the plume moves downwind (birds eye view at 1200 m above ground). The dilution of the plume can be

25   seen in the ΔCO values as high as 16,000 ppbv between the center of the plume within the first hour after initial emission to five hours downwind, where the plume was modeled to be approximately 100 km wide, with an average in-plume ΔCO concentration of approximately 1000 ppbv. Figure 2 shows a vertical slice of (looking into) the plume at 1, 2, and 5 hours downwind for ΔCO, $\Delta O_3/\Delta CO$ and $\Delta OA/\Delta CO_2$, and these results will be discussed in the following sections. Note that ΔCO_2 was used to as the NEMR denominator, as in Alvarado et al. (2015), so as to more easily compare model results.

30   4.1 Gas-phase Simulations

The in-plume CO enhancement ($\Delta CO = CO_{\text{in-plume}} - CO_{\text{background}}$, in ppbv) and NEMRs (Eq. 1) for O_3, are shown in Figures 2 and 3. PAN, NO_x, HONO and NH_3 are shown in just Figure 3, where the average NEMR across SAM-ASP v1.0 grid boxes is calculated where the CO concentrations are above a background threshold of 150 ppbv (based on measurements). In Figure 3, horizontal error bars indicate the age uncertainty of the measurements, with a best estimate of the starting NEMR and uncertainty discussed in

35   Akagi et al. (2012), which uses a slope-based fire-average ER as a best estimate of the likely starting NEMR for primary species measured in individual smoke transects. The SAM-ASP v1.0 model was qualitatively able to simulate the dilution of CO in the

smoke plume after 2 hours to within the uncertainties of the measurements but with an underestimate of dispersion in the first two hours. SAM-ASP v1.0 also correctly simulated the chemical loss of NO_x and HONO and formation of PAN and O_3 within the plume. After two hours of model simulated O_3 (second row in Figure 2), it can be seen that the edges of the plume have higher concentrations than the center, a feature that cannot be represented in a box model simulation. This O_3 enhancement at the edges may be a result of less NO titration at the plume edges. We expect larger O_3 edge effects in future work when the TUV radiation model is coupled online and interacts with plume aerosols. NH_3 concentrations in the model were overestimated (model value of $\Delta NH_3/\Delta CO$ of 0.04 ppb ppb^{-1} at 5 h, rather than the measured value of 0.02 mol mol^{-1}). This is in contrast to the results of the ASP Lagrangian box model study of Alvarado et al. (2015), where the box model simulated NH_3 closer to measured values at all hours downwind. The lack of vertical variation in the SAM-ASP plume in Figure 3 may be due to the use of constant photolysis rates in this version of SAM-ASP, with future work needed to incorporate in-line photolysis consideration.

4.2 Aerosol Simulations

OA NEMR results from the ASP box model (Alvarado et al., 2015) and measurements from Akagi et al. (2012) are compared to cross-plume-averaged SAM-ASP output in Figure 4. In general, the SAM-ASP results show slightly slower initial dilution than the box model, with the initial increase in OA due to the 2D wall staying over the emission area, thus evaporative driven decreases have not dominated yet. This difference in dilution rate, and thus OA NEMR, is due to dilution in the box being forced to match measurements while in SAM-ASP, the meteorology and initial plume width determine the relative dispersion rate (Alvarado et al., 2015). Within the first hour after emission, SAM-ASP has less dilution than the box model (Figure 3a and 4), leading to a higher OA concentration, which in turn leads to less evaporation of OA to intermediate and semi-volatile vapors, explaining the larger OA NEMR for this initial time period. However, SAM-ASP has greater dilution than the box model after 2 hours (though both falling within measurement uncertainties in Figure 3a), which lead to more OA evaporation in SAM-ASP than in the box model, leading to a lower OA NEMR after 2 hours, better matching the measurements. We note, however, that there are considerable uncertainties in the volatility distribution of the simulated POA as well as the SOA chemistry, so there may be multiple ways to improve modeled OA NEMR. The bottom panels of Figure 2 shows that the OA NEMR in the model initially decreases faster than the core, driven by dilution. However, after several hours the OA NEMR at the edges increases, showing that SOA production in those locations is exceeding evaporation in those locations. This initial evaporation followed by net SOA production is consistent with the theoretical studies of Bian et al. (2017) and Hodshire et al. (2019b); however, those studies did not explore this behavior in the plume edges versus the core. SAM-ASP will be used in future work to investigate these plume edge versus core differences within field observations.

We also compared the predictions for aerosol size distribution changes between the two models (Figure 5). Note that as no size distribution measurements were taken for this fire, we cannot compare these simulations with observations. The top plot shows the average size distribution of the background air in the SAM-ASP simulation. We again average the SAM-ASP results across grid boxes where CO concentration are above the CO threshold (150 ppbv) in each timestep. Both models suggest that this fire showed little net aerosol diameter growth (bottom two plots), as shrinking due to evaporative losses driven by dilution compensates growth by coagulation and the oxidation (and reduction in volatility) of the organic vapors, consistent with the OA NEMR results above.

5 Conclusions

The newly coupled SAM-ASP model allows for a detailed examination of the chemical and physical evolution of fine-scale biomass burning plumes. SAM-ASP is able to simulate the complex, non-linear production of O_3 and changes in PM as plumes age. It is able to resolve the cross-plume chemistry, gas-to-particle partitioning, and microphysics that coarser grid-scale CTMs

5   are not able to. Model results indicate SAM-ASP is able to accurately simulate the dilution of CO in a California chaparral smoke plume mostly, except for a slight initial underprediction, as well as accurately predict the chemical loss of NO_x and HONO and production of O_3 and PAN within the plume. SAM-ASP also resolves the cross-plume concentration of trace-gases and aerosol. Future work will involve testing SAM-ASP simulations against observed plume crosswind and vertical gradients as well as size distributions. Future work will also include the development of a biomass burning parameterization of plume-scale chemical and

10   physical trace gas and aerosol evolution for use in coarser grid-scale CTMs (that cannot resolve plumes) as well as the implementation of on-line photolysis calculations to explicitly simulate the effect of in-plume aerosols on photolysis rates.

6 Data Availability

SAM-ASP 1.0 source code is available for download through the SAM website at http://rossby.msrc.sunysb.edu/~marat/SAM.html through request to the SAM model developer, Dr. Marat Khairoutdinov. Separate ASP model code, model inputs, outputs and

15   post-processing steps described in this study are available in a public repository at https://doi.org/10.5281/zenodo.3363995, doi: 10.5281/zenodo.3363995.

Competing Interests. The authors declare they have no conflicts of interest.

20   *Author Contribution.* C.R. Lonsdale provided the design and performed the execution of the model implementation, simulation and evaluation of the SAM-ASP code and prepared this manuscript. M. J. Alvarado and J. R. Pierce provided oversight and leadership of the overall development and acquired the financial support for the project leading to this publication, as well as contributed to the review and editing of this manuscript. A. L. Hodshire and E. Ramnarine provided verification of the overall reproducibility of model results, presented complementary published work and contributed to the review and editing of this

25   manuscript.

Acknowledgements. We would like to thank Dr. Marat Khairoutdinov for hosting the SAM-ASP model code. This work was supported by NOAA Atmospheric Chemistry, Carbon Cycle and Climate Program awards #NA17OAR430001 and #NA17OAR4310002 and NSF Atmospheric Chemistry Program Grants #1559598 and #1559607 as well as by the State of Texas

30   through the Air Quality Research Program administered by The University of Texas at Austin by means of a Grant from the Texas Commission on Environmental Quality.

7 References

Ahmadov, R., McKeen, S. A., Robinson, A. L., Bahreini, R., Middlebrook, A. M., de Gouw, J. A., Meagher, J., Hsie, E.-Y., Edgerton, E., Shaw, S., and Trainer, M.: A volatility basis set model for summertime secondary organic aerosols over the eastern United States in 2006, J. Geophys. Res., 117, 2156–2202, 2012.

Akagi, S. K., Yokelson, R. J., Wiedinmyer, C., Alvarado, M. J., Reid, J. S., Karl, T., Crounse, J. D., and Wennberg, P. O.: Emission factors for open and domestic biomass burning for use in atmospheric models, Atmos. Chem. Phys., 11, 4039–4072, https://doi.org/10.5194/acp-11-4039-2011, 2011.

Akagi, S. K., Craven, J. S., Taylor, J. W., McMeeking, G. R., Yokelson, R. J., Burling, I. R., Urbanski, S. P., Wold, C. E., Seinfeld, J. H., Coe, H., Alvarado, M. J., and Weise, D. R.: Evolution of trace gases and particles emitted by a chaparral fire in California, Atmos. Chem. Phys., 12, 1397–1421, 2012.

Alvarado, M. J.: Formation of ozone and growth of aerosols in young smoke plumes from biomass burning, Ph.D. thesis, Massachusetts Institute of Technology, Cambridge, MA, USA, 324 pp., available at http://globalchange.mit.edu/files/document/ Alvarado_PhD_08.pdf, 2008.

Alvarado, M. J., and Prinn, R. G.: Formation of ozone and growth of aerosols in young smoke plumes from biomass burning, Part 1: Lagrangian parcel studies, J. Geophys. Res., 114, D09306, 2009.

Alvarado, M. J., Wang, C., and Prinn, R. G.: Formation of ozone and growth of aerosols in young smoke plumes from biomass burning, Part 2: 3D Eulerian studies, J. Geophys. Res., 114, D09307, https://doi.org/10.1029/2008JD011186, 2009.

Alvarado, M. J., Logan, J. A., Mao, J., Apel, E., Riemer, D., Blake, D., Cohen, R. C., Min, K.-E., Perring, A. E., Browne, E. C., Wooldridge, P. J., Diskin, G. S., Sachse, G. W., Fuelberg, H., Sessions, W. R., Harrigan, D. L., Huey, G., Liao, J., Case-Hanks, A., Jimenez, J. L., Cubison, M. J., Vay, S. A., Weinheimer, A. J., Knapp, D. J., Montzka, D. D., Flocke, F. M., Pollack, I. B., Wennberg, P. O., Kurten, A., Crounse, J., Clair, J. M. St., Wisthaler, A., Mikoviny, T., Yantosca, R. M., Carouge, C. C., and Le Sager, P.: Nitrogen oxides and PAN in plumes from boreal fires during ARCTAS-B and their impact on ozone: an integrated analysis of aircraft and satellite observations, Atmos. Chem. Phys., 10, 9739–9760, https://doi.org/10.5194/acp-10-9739-2010, 2010.

Alvarado, M. J., Lonsdale, C. R., Yokelson, R. J., Akagi, S. K., Coe, H., Craven, J. S., Fischer, E. V., McMeeking, G. R., Seinfeld, J. H., Soni, T., Taylor, J. W., Weise, D. R., and Wold, C. E.: Investigating the links between ozone and organic aerosol chemistry in a biomass burning plume from a prescribed fire in California chaparral, Atmos. Chem. Phys., 15, 6667–6688, https://doi.org/10.5194/acp-15-6667-2015, 2015.

Alvarado, M. J., Lonsdale, C. R., Macintyre, H. L., Bian, H., Chin, M., Ridley, D. A., Heald, C. L., Thornhill, K. L., Anderson, B. E., Cubison, M. J., Jimenez, J. L., Kondo, Y., Sahu, L. K., Dibb, J. E., and Wang, C.: Evaluating model parameterizations of submicron aerosol scattering and absorption with in situ data from ARCTAS 2008, Atmos. Chem. Phys., 16, 9435-9455, https://doi.org/10.5194/acp-16-9435-2016, 2016.

Bais, A. F., Madronich, S., Crawford, J., Hall, S. R., Mayer, B., van Weele, M., Lenoble, J., Calvert, J. G., Cantrell, C. A., Shetter, R. E., Hofzumahaus, A., Koepke, P., Monks, P. S., Frost, G., McKenzie, R., Krotkov, N., Kylling, A., Swartz, W. H., Lloyd, S., Pfister, G., Martin, T. J., Roeth, E., Griffioen, E., Ruggaber, A., Krol, M., Kraus, A., Edwards, G. D., Mueller, M., Lefer, B. L., Johnston, P., Schwander, H., Flittner, D., Gardiner, B. G., Barrick, J., and Schmitt, R.: International photolysis frequency measurement and model intercomparison: Spectral actinic solar flux measurements and modeling, J. Geophys. Res., 2003, 108, 8543.

Baker, K.: Simulating fire event impacts on regional O3 and PM2.5 and looking toward evaluation, 14th Annual CMAS Conference, UNC-Chapel Hill, 5–7 October, 2015.

Baylon, P., Jaffe, D., Hall, S., Ullmann, K., Alvarado, M., Lefer, B., 2018. Impact of Biomass Burning Plumes on Photolysis Rates and Ozone Formation at the Mount Bachelor Observatory. Journal of Geophysical Research: Atmospheres 123, 2272–2284.

Bian, H., Chin, M., Hauglustaine, D. A., Schulz, M., Myhre, G., Bauer, S. E., Lund, M. T., Karydis, V. A., Kucsera, T. L., Pan, X., Pozzer, A., Skeie, R. B., Steenrod, S. D., Sudo, K., Tsigaridis, K., Tsimpidi, A. P., and Tsyro, S. G.: Investigation of global particulate nitrate from the AeroCom phase III experiment, Atmos. Chem. Phys., 17, 12911–12940, https://doi.org/10.5194/acp-17-12911-2017, 2017.

Bond, T. C., Doherty, S. J., Fahey, D. W., Forster, P. M., Berntsen, T., DeAngelo, B. J., Flanner, M. G., Ghan, S., Kärcher, B., Koch, D., Kinne, S., Kondo, Y., Quinn, P. K., Sarofim, M. C., Schultz, M. G., Schulz, M., Venkataraman, C., Zhang, H., Zhang, S., Bellouin, N., Guttikunda, S. K., Hopke, P. K., Jacobson, M. Z., Kaiser, J. W., Klimont, Z., Lohmann, U., Schwarz, J. P., Shindell, D., Storelvmo, T., Warren, S. G., and Zender, C. S.: Bounding the role of black carbon in the climate system: A scientific assessment., J. Geophys. Res. Atmos., 118, 5380–5552, 2013.

Boucher, O., Randall, D., Artaxo, P., Bretherton, C., Feingold, G., Forster, P., Kerminen, V.-M., Kondo, Y., Liao, H., Lohmann, U., Rasch, P., Satheesh, S. K., Sherwood, S., Stevens, B., and Zhang, X. Y.: Climate Change 2013: The Physical Science Basis. Contribution of Working Group I to the Fifth Assessment Report of the Intergovernmental Panel on Climate Change, edited by: Stocker, T. F., Qin, D., Plattner, G.-K., Tignor, M., Allen, S. K., Boschung, J., Nauels, A., Xia, Y., Bex, V., and Midgley, P. M., Cambridge University Press, 2013.

Collier, S., Zhou, S., Onasch, T. B., Jaffe, D. A., Kleinman, L., Sedlacek, A. J. III, Briggs, N. L., Hee, J., Fortner, E., Shilling, J. E., Worsnop, D., Yokelson, R. J., Parworth, C., Ge, X., Xu, J., Butterfield, Z., Chand, D., Dubey, M. K., Pekour, M. S., Springston, S., and Zhang, Q.: Regional influence of aerosol emissions from wildfires driven by combustion efficiency: Insights from the BBOP campaign, Environ. Sci. Tech., 50(16), 8613–8622, 2016.

Crounse, J. D., Knap, H. C., Ørnsø, K. B., Jørgensen, S., Paulot, F., Kjaergaard, H. G., and Wennberg, P. O.: Atmospheric fate of methacrolein. 1. Peroxy radical isomerization following addition of OH and O2, J. Phys. Chem. A, 116, 5756–5762, https://doi.org/10.1021/jp211560u, 2012.

European Environment Agency. Air quality in Europe - 2018 report. Available at: https://www.eea.europa.eu/publications/air-quality-in-europe-2018/download (Accessed 02 May 2019), 2018.

Fan, J., Ovtchinnikov, M., Comstock, J. M., McFarlane, S. A., and Khain, A.: Ice formation in Arctic mixed-phase clouds: Insights from a 3-D cloud-resolving model with size-resolved aerosol and cloud microphysics, J. Geophys. Res. Atmos., 114, 2009.

Flynn, J., Lefer, B., Rappenglück, B., Leuchner, M., Perna, R., Dibb, J., Ziemba, L., Anderson, C., Stutz, J., Brune, W., Ren, X., Mao, J., Luke, W., Olson, J., Chen, G., and Crawford, J.: Impact of clouds and aerosols on ozone production in Southeast Texas, Atmos. Environ., 44(33), 4126–4133. https://doi.org/10.1016/j.atmosenv.2009.09.005, 2010.

Goliff, W. S., Stockwell, W. R., and Lawson, C. V.: The regional atmospheric chemistry mechanism, version 2, Atmos. Environ., 68, 174–185, 2013.

Grieshop, A. P., Logue, J. M., Donahue, N. M., and Robinson, A. L.: Laboratory investigation of photochemical oxidation of organic aerosol from wood fires 1: measurement and simulation of organic aerosol evolution, Atmos. Chem. Phys., 9, 1263–1277, https://doi.org/10.5194/acp-9-1263-2009, 2009a.

Grieshop, A. P., Donahue, N. M., and Robinson, A. L.: Laboratory investigation of photochemical oxidation of organic aerosol from wood fires 2: analysis of aerosol mass spectrometer data, Atmos. Chem. Phys., 9, 2227–2240, https://doi.org/10.5194/acp-9-2227-2009, 2009b.

Hess, M., Koepke, P., and Schult, I.: Optical Properties of Aerosols and clouds: The software package OPAC, B. Am. Meteorol. Soc., 79, 831–844, 1998.

Hobbs, P. V., P. Sinha, R. J. Yokelson, T. J. Christian, D. R. Blake, S. Gao, T. W. Kirschstetter, T. Novakov, and P. Pilewskie, Evolution of gases and particles from a savanna fire in South Africa, J. Geophys. Res., 108(D13), 8485,
5   doi:10.1029/2002JD002352, 2003.

Hodshire, A. L., Akherati, A., Alvarado, M. J., Brown-Steiner, B., Jathar, S. H., Jimenez, J. L., Kreidenweis, S. M., Lonsdale, C. R., Onasch, T. B., Ortega, A. M., Pierce, J. R.,: Aging Effects on Biomass Burning Aerosol Mass and Composition: A Critical Review of Field and Laboratory Studies, Env. Sci. Tech., https://doi.org/10.1021/acs.est.9b02588, 2019a.

Hodshire, A. L., Bian, Q., Ramnarine, E., Lonsdale, C. R., Alvarado, M. J., Kreidenweis, S. M., Jathar, S. H., and Pierce, J. R.:
10   More than emissions and chemistry: Fire size, dilution, and background aerosol also greatly influence near-field biomass burning aerosol aging, J. Geophys. Res., 124, https://doi.org/10.1029/2018JD029674, 2019b.

Hosseini, S., Li, Q., Cocker, D., Weise, D., Miller, A., Shrivastava, M., Miller, J. W., Mahalingam, S., Princevac, M., and Jung, H.: Particle size distributions from laboratory-scale biomass fires using fast response instruments, Atmos. Chem. Phys., 10, 8065–8076 (2010).

15 Jacob, D. J.: Heterogeneous chemistry and tropospheric ozone, Atmos. Environ., 34, 2131–2159, 2000.

Jacobson, M. Z., Analysis of aerosol interactions with numerical techniques for solving coagulation, nucleation, condensation, dissolution, and reversible chemistry among multiple size distributions, J. Geophys. Res., 107(D19), 4366, doi:10.1029/2001JD002044, 2002.

Jacobson, M. Z.: Fundamentals of Atmospheric Modelling, 2nd ed., Cambridge University Press, 2005.

20 Janhäll, S., Andreae, M., and Pöschl, U.: Biomass burning aerosol emissions from vegetation fires: particle number and mass emission factors and size distributions., Atmos. Chem. Phys., 1427–1439, 2010.

Jenkin, M. E., Saunders, S. M., Wagner, V., and Pilling, M. J.: Protocol for the development of the Master Chemical Mechanism, MCM v3 (Part B): tropospheric degradation of aromatic volatile organic compounds, Atmos. Chem. Phys., 3, 181–193, https://doi.org/10.5194/acp-3-181-2003, 2003.

25 Khairoutdinov, M. F., and Randall, D. A.: Cloud resolving modeling of the ARM summer 1997 IOP: Model formulation, results, uncertainties, and sensitivities, J. Atmos. Sci., 60, 607–625, 2003.

Knorr, W., Dentener, F., Lamarque, J.-F., Jiang, L., and Arneth, A.: Wildfire air pollution hazard during the 21st century, Atmos. Chem. Phys., 17, 9223–9236, https://doi.org/10.5194/acp-17-9223-2017, 2017.

Lee, L. A., Pringle, K. J., Reddington, C. L., Mann, G. W., Stier, P., Spracklen, D. V., Pierce, J. R., and Carslaw, K. S.: The
30   magnitude and causes of uncertainty in global model simulations of cloud condensation nuclei, Atmos. Chem. Phys., 13, 8879–8914, https://doi.org/10.5194/acp-13-8879-2013, 2013.

Lonsdale, C. R., Stevens, R. G., Brock, C. A., Makar, P. A., Knipping, E. M., and Pierce, J. R.: The effect of coal-fired power-plant SO_2 and NO_x control technologies on aerosol nucleation in the source plumes, Atmos. Chem. Phys., 12, 11519–11531, https://doi.org/10.5194/acp-12-11519-2012, 2012.

35 Lonsdale, C. R., Alvarado, M. J., Yokelson, R. J., Akagi, S. K., Fischer, E., Travis, K., Soni, T., Craven, J. S., Taylor, J. W., McMeeking, G. R., Burling, I. R., Urbanski, S. P., Wold, C. E., Seinfeld, J. H., Coe, H., and Weise, D. R.: Modeling the Chemistry and Growth of Organic Aerosol in Biomass Burning Plumes at Local and Regional Scales, American Association for Aerosol Research, Minneapolis, MN, October 12-16, 2015.

Magi, B. I., and Hobbs, P. V.: Effects of humidity on aerosols in southern Africa during the biomass burning season, J. Geophys.
40   Res., 108(D13), 8495, https://doi.org/10.1029/2002JD002144, 2003.

Maxwell Garnet, J. C.: Colours in metal glasses and in metallic films, Philos. T. R. Soc. A, 203, 385–420, 1904.

McClure, C. D., and Jaffe, D. A. 2018. U.S. particulate matter air quality improves except in wildfire-prone areas. PNAS , DOI: 10.1073/pnas.1804353115.

McDonald-Buller, E., Kimura, Y., Wiedinmyer, C., Emery, C., Liu, Z., and Yarwood G.: Targeted Improvements in the Fire Inventory form NCAR (FINN) Model for Texas Air Quality Planning, Final Report to Texas Air Quality Research Program (AQRP) for Project 14-011, December 2015.

Messinger, F., DiMego, G., Kalnay, E., Mitchell, K., Shafran, P. C., Ebisuzaki, W., Jović, D., Woollen, J., Rogers, E., Berbery, E. H., and Ek, M. B.: North American regional reanalysis, Bull. Am. Met. Soc., 87(3), 343–360, 2006.

O'Dell, K., Ford, B., Fischer, E., and Pierce, J. (2019). The contribution of wildland-fire smoke to US PM 2.5 and its influence on recent trends. Environ. Sci. Techn. 53. 10.1021/acs.est.8b05430.

Ordóñez, C., Elguindi, N., Stein, O., Huijnen, V., Flemming, J., Inness, A., Flentje, H., Katragkou, E., Moinat, P., Peuch, V.-H., Segers, A., Thouret, V., Athier, G., van Weele, M., Zerefos, C. S., Cammas, J.-P., and Schultz, M. G.: Global model simulations of air pollution during the 2003 European heat wave, Atmos. Chem. Phys., 10, 789–815, https://doi.org/10.5194/acp-10-789- 2010, 2010.

Ovchinnikov, M., Ackerman, A. S., Avramov, A., Cheng, A., Fan, J., Fridlind, A. M., Ghan, S., Harrington, J., Hoose, C., Korolev, A., McFarquhar, G. M., Morrison, H., Paukert, M., Savre, J., Shipway, B. J., Shupe, M. D., Solomon, A., and Sulia, K.: Intercomparison of large-eddy simulations of Arctic mixed-phase clouds: Importance of ice size distribution assumptions, J. Adv. Model. Earth Sys., 6(1), 223–248, 2014.

Paulot, F., Crounse, J. D., Kjaergaard, H. G., Kroll, J. H., Seinfeld, J. H., and Wennberg, P. O.: Isoprene photooxidation: new insights into the production of acids and organic nitrates, Atmos. Chem. Phys., 9, 1479–1501, doi:10.5194/acp-9-1479-2009, 2009a.

Paulot, F., Crounse, J. D., Kjaergaard, H. G., Kurten, A., St. Clair, J. M., Seinfeld, J. H., and Wennberg, P. O.: Unexpected epoxide formation in the gas-phase photooxidation of isoprene, Science, 325, 730–733, https://doi.org/10.1126/science.1172910, 2009b.

Petters, M. D., and Kreidenweis, S. M.: A single parameter representation of hygroscopic growth and cloud condensation nucleus activity, Atmos. Chem. Phys., 7, 1961–1971, https://doi.org/10.5194/acp-7-1961-2007, 2007.

Pierce, J. R., Chen, K., and Adams, P. J.: Contribution of primary carbonaceous aerosol to cloud condensation nuclei: processes and uncertainties evaluated with a global aerosol microphysics model, Atmos. Chem. Phys., 7, 5447–5466, https://doi.org/10.5194/acp-7- 5447-2007, 2007.

Ramnarine, E., Kodros, J. K., Hodshire, A. L., Lonsdale, C. R., Alvarado, M. J., and Pierce, J. R.: Effects of near-source coagulation of biomass burning aerosols on global predictions of aerosol size distributions and implications for aerosol radiative effects, Atmos. Chem. Phys., 19, 6561–6577, https://doi.org/10.5194/acp-19-6561-2019, 2019.

Reid, J. S., Koppmann, R., Eck, T. F., and Eleuterio, D. P.: A review of biomass burning emissions. Part II: Intensive physical properties of biomass burning particles, Atmos. Chem. Phys., 5, 799–825, 2005.

Robinson, A. L., Donahue, N. M., Shrivastava, M. K., Weitkamp, E. A., Sage, A. M., Grieshop, A. P., Lane, T. E., Pierce, J. R., and Pandis, S. N.: Rethinking organic aerosols: semivolatile emissions and photochemical aging, Science, 315, 1259–1262, 2007.

Sakamoto, K. M., Allan, J. D., Coe, H., Taylor, J. W., Duck, T. J., and Pierce, J. R.: Aged boreal biomass-burning aerosol size distributions from BORTAS 2011, Atmos. Chem. Phys., 15, 1633–1646, https://doi.org/10.5194/acp-15-1633-2015, 2015.

Sakamoto, K. M., Laing, J. R., Stevens, R. G., Jaffe, D. A., and Pierce, J. R.: The evolution of biomass-burning aerosol size distributions due to coagulation: dependence on fire and meteorological details and parameterization, Atmos. Chem. Phys., 16, 7709–7724, https://doi.org/10.5194/acp-16-7709-2016, 2016.

Seinfeld, J.H. and Pandis, S.N. (2016) Atmospheric Chemistry and Physics: From Air Pollution to Climate Change. John Wiley
5   & Sons, Hoboken.

Spracklen, D. V., Carslaw, K. S., Pöschl, U., Rap, A., and Forster, P. M.: Global cloud condensation nuclei influenced by carbonaceous combustion aerosol, Atmos. Chem. Phys., 11, 9067–9087, https://doi.org/10.5194/acp-11-9067-2011, 2011.

Stevens, R. G., Pierce, J. R., Brock, C. A., Reed, M. K., Crawford, J. H., Holloway, J. S., Ryerson, T. B., Huey, L. G., and Nowak, J. B.: Nucleation and growth of sulfate aerosol in coal-fired power plant plumes: sensitivity to background aerosol
10   and meteorology, Atmos. Chem. Phys., 12, 189–7206, https://doi.org/10.5194/acp-12-189-2012, 2012.

Stevens, R. G., and Pierce, J. R.: The contribution of plume-scale nucleation to global and regional aerosol and CCN concentrations: evaluation and sensitivity to emissions changes, Atmos. Chem. Phys., 14, 13661–13679, https://doi.org/10.5194/acp-14-13661-2014, 2014.

Stockwell, C. E., Yokelson, R. J., Kreidenweis, S. M., Robinson, A. L., DeMott, P. J., Sullivan, R. C., Reardon, J., Ryan, K. C.,
15   Griffith, D. W. T., and Stevens, L.: Trace gas emissions from combustion of peat, crop residue, domestic biofuels, grasses, and other fuels: configuration and Fourier transform infrared (FTIR) component of the fourth Fire Lab at Missoula Experiment (FLAME-4), Atmos. Chem. Phys., 14, 9727–9754, https://doi.org/10.5194/acp-14-9727-2014, 2014.

Tang, I. N.: Thermodynamic and optical properties of mixed-salt aerosols of atmospheric importance, J. Geophys. Res., 102(D2), 1883, 1997.

20 Toon, O. B., and Ackerman, T. P.: Algorithms for the calculation of scattering by stratied spheres, Appl. Opt., 20, 3657–3660, https://doi.org/10.1364/AO.20.003657, 1981.

U.S. EPA. Integrated Science Assessment (ISA) of Ozone and Related Photochemical Oxidants (Final Report, Feb 2013). U.S. Environmental Protection Agency, Washington, DC, EPA/600/R-10/076F, 2013.

Wentworth, G. R., Aklilu, Y., Landis, M. S., and Hsu,Y. M.: Impacts of a large boreal wildfire on ground level atmospheric
25   concentrations of PAHs, VOCs and ozone, Atmos. Environ., 178, 19–30, 2018.
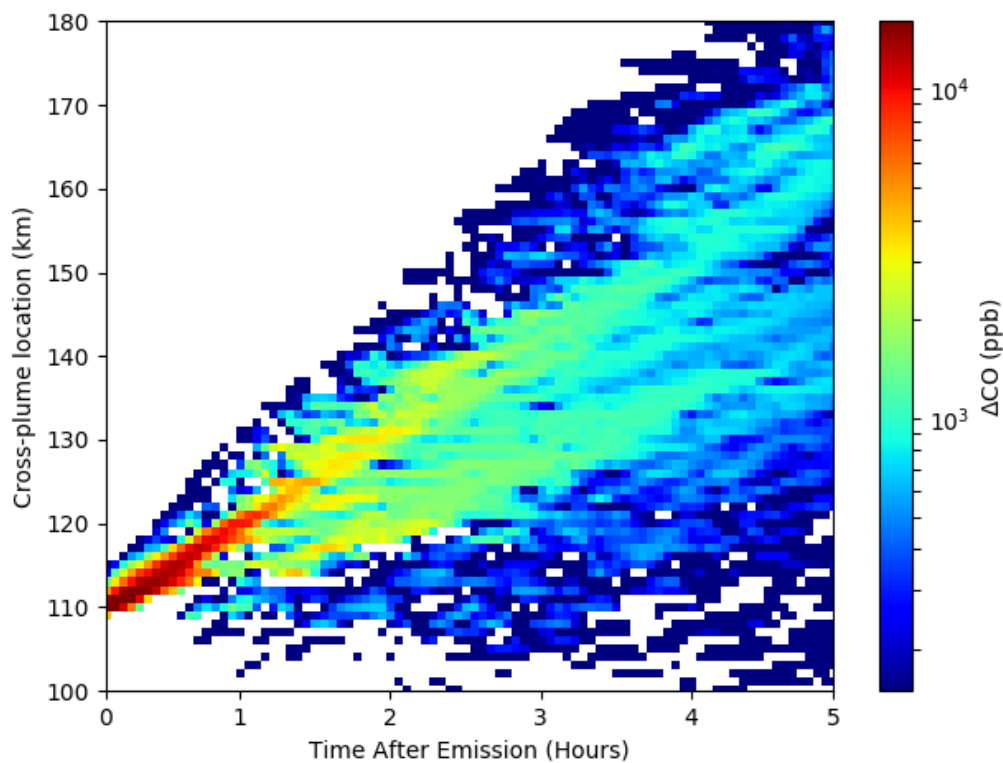
Figure 1. SAM-ASP Williams fire simulation of cross-plume location versus time since emission at a vertical height of 1200 m for ΔCO.
5 **Note that figure is zoomed in on the plume with white background indicating a CO concentration less than 150 ppb.**
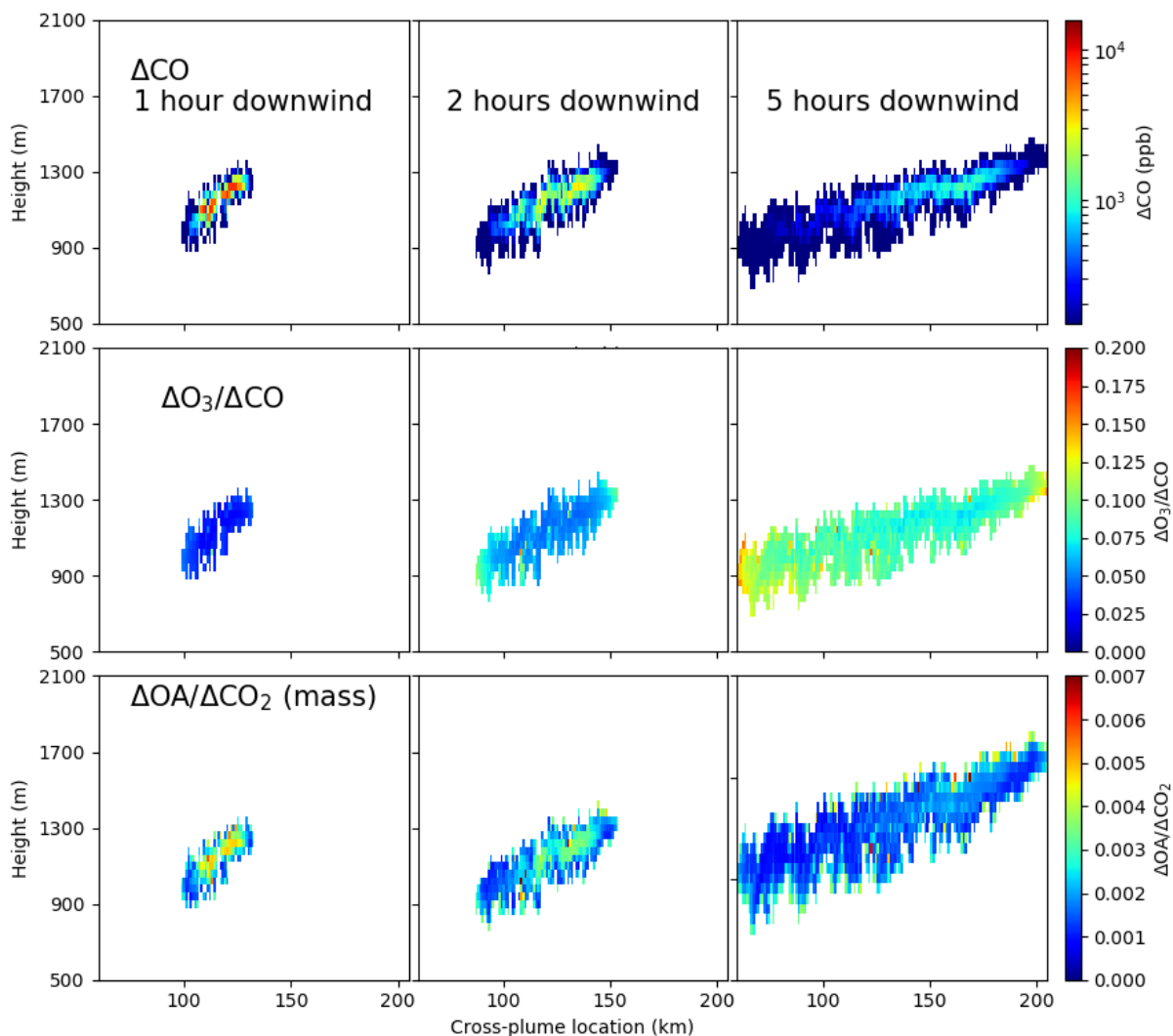
Figure 2. Height vs cross-plume location at 1 hour (left column), 2 hours (center column) and 5 hours (right column) downwind of fire source for ΔCO (top row), $\Delta O_3/\Delta CO$ (ppb/ppb, center row) and $\Delta OA/\Delta CO_2$ (bottom row). Note that figure is zoomed in on the plume and white indicates a CO concentration less than 150 ppb.
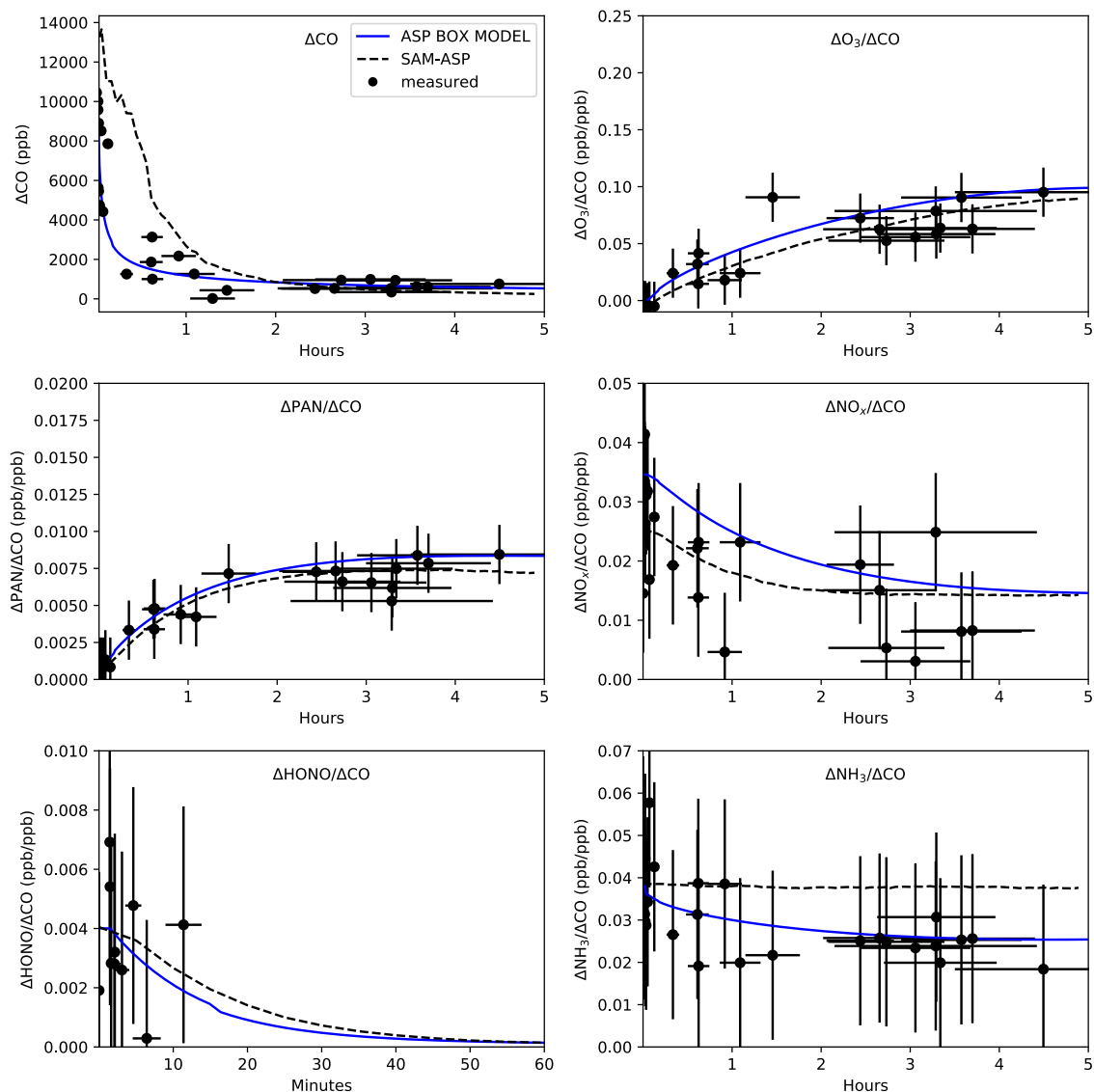
Figure 3. Cross-plume averaged ΔCO and O₃, PAN, NOₓ, HONO and NH₃ NEMRs (ΔX/ΔCO) as a function of plume age for the ASP box model (solid line) and SAM-ASP model (dashed-line) results compared to measurements from Akagi et al. (2012) (dots).
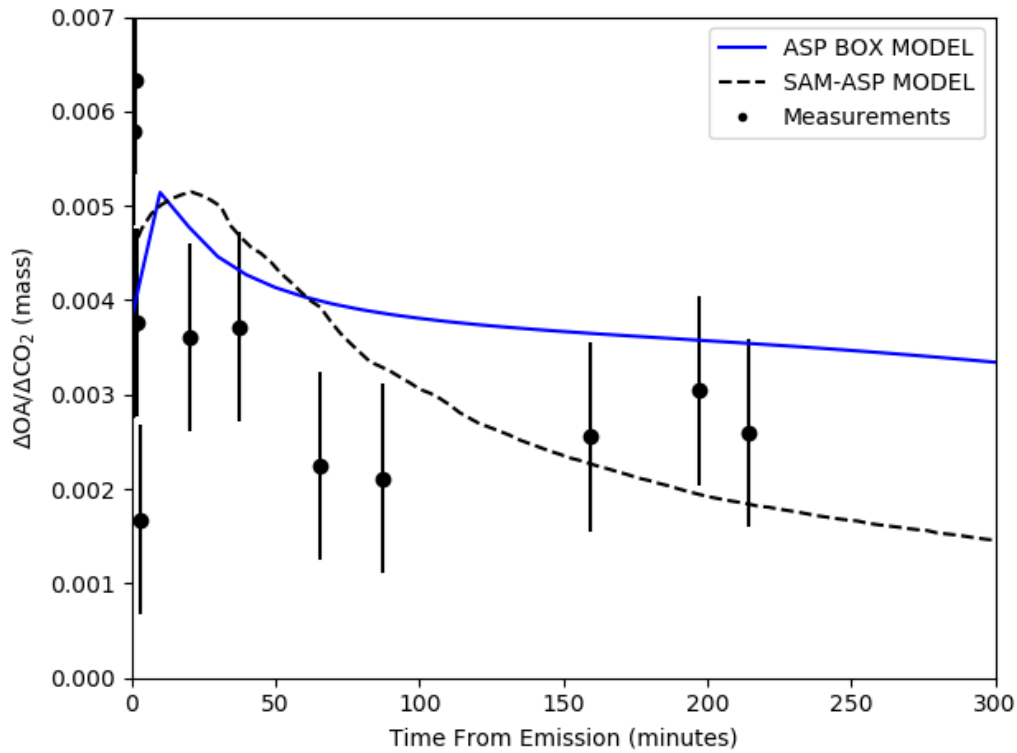
Figure 4. Cross-plume averaged OA NEMR (ΔOA/ΔCO₂) for the Williams fire from SAM-ASP simulations (dashed line), the ASP box model results as described in Alvarado et al. (2015) (solid lines), and OA measurements (back dots) described in Akagi et al., (2012).
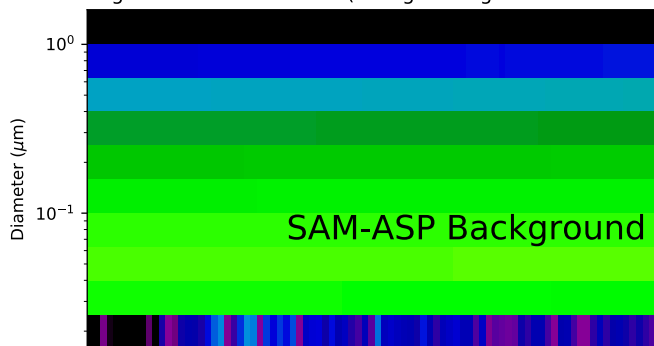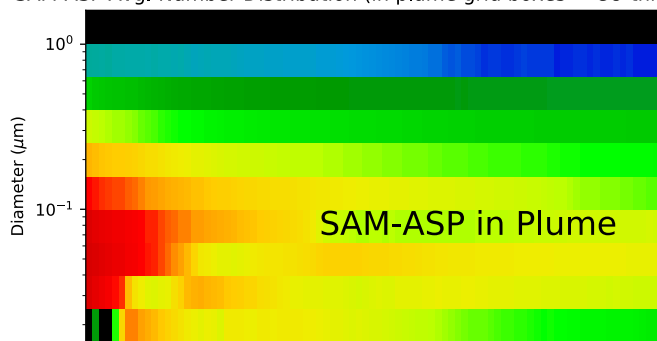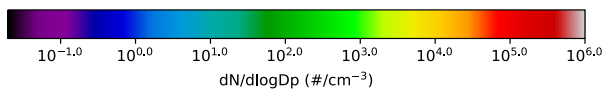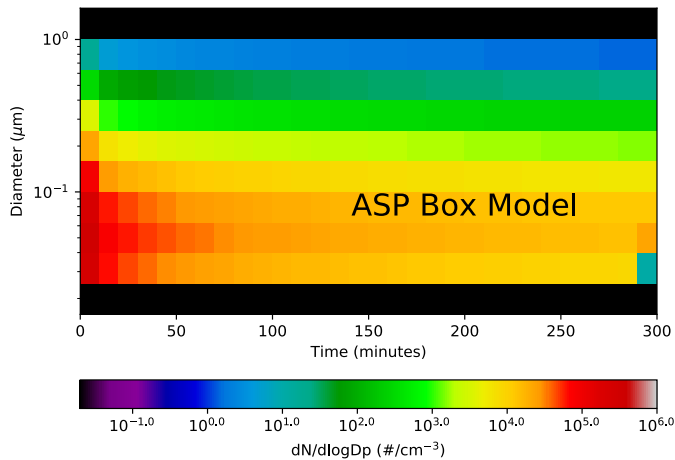
Figure 5. SAM-ASP (top) and ASP box model (bottom) simulated particle size distribution (dN/dlogD$_p$ cm^{-3}) evolution within the Williams fire.